Lattice Study of the Dibaryon System

Zi-Yu Wang, In Collaboration: Xu Feng (PKU), Luchang Jin (University of Connecticut)

2021.7.27

Peking University

Contents

Introduction

Introduction

- Some of the dibaryon weak transition matrix elements: $\langle de^+\nu_e \,|\, \mathcal{O}^- \,|\, pp\rangle$, $\langle ppee\bar{\nu}_e\bar{\nu}_e \,|\, \mathcal{O}^+\mathcal{O}^+ \,|\, nn\rangle$, $\langle ppee \,|\, \mathcal{O}^+\mathcal{O}^+ \,|\, nn\rangle$
- Important probes of SM and BSM physics, especially $0\nu2\beta$.
- Providing theoretical LECs for effective theories.
- Pioneering calculation of $pp \to d$ and $2\nu2\beta$ has been performed by NPLQCD. (Savage et al. 2017; Tiburzi et al. 2017)
- We will present our methodology and preliminary results.

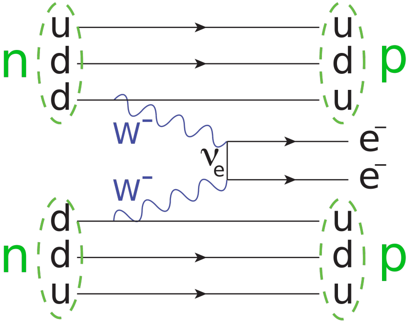

Figure 1: $0\nu2\beta$

Methodology

Dibaryon Interpolating Fields

Two Kinds of Correlators

- Point source & sink (PP) vs. Split Point source & sink (SPSP).

Why SPSP?

- PP $\rightarrow$ High-momentum states contamination.

$$\sum_{\boldsymbol{x}} C(x;x_0) \propto \sum_{\boldsymbol{x},\boldsymbol{p},\boldsymbol{k}} \tilde{S}(p)\tilde{S}(k)\mathrm{e}^{-\mathrm{i}(\boldsymbol{p}+\boldsymbol{k})\cdot\boldsymbol{x}} = \sum_{\boldsymbol{p}} \tilde{S}(E,\boldsymbol{p})\tilde{S}(E,-\boldsymbol{p})$$

- SPSP $\rightarrow$ High-momentum states are suppressed.

$$\sum_{\boldsymbol{x},\boldsymbol{y}} C(x,y;x_0,y_0) \propto \sum_{\substack{\boldsymbol{x},\boldsymbol{y}\\ \boldsymbol{p},\boldsymbol{k}}} \tilde{S}(p)\tilde{S}(k)\mathrm{e}^{-\mathrm{i}(\boldsymbol{p}\cdot\boldsymbol{x}+\boldsymbol{k}\cdot\boldsymbol{y})} = \tilde{S}(E,\vec{0})\tilde{S}(E,\vec{0})$$

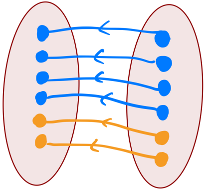

PP

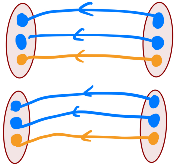

SPSP

Dibaryon Interpolating Fields

Two Kinds of Correlators

- Point source & sink (PP) vs. Split Point source & sink (SPSP).

Why SPSP?

- PP $\rightarrow$ High-momentum states contamination.

$$\sum_{\boldsymbol{x}} C(x; x_0) \propto \sum_{\boldsymbol{x},\boldsymbol{p},\boldsymbol{k}} \tilde{S}(p)\tilde{S}(k)\mathrm{e}^{-\mathrm{i}(\boldsymbol{p}+\boldsymbol{k})\cdot\boldsymbol{x}} = \sum_{\boldsymbol{p}} \tilde{S}(E,\boldsymbol{p})\tilde{S}(E,-\boldsymbol{p})$$

- SPSP $\rightarrow$ High-momentum states are suppressed.

$$\sum_{\boldsymbol{x},\boldsymbol{y}} C(x, y; x_0, y_0) \propto \sum_{\substack{\boldsymbol{x},\boldsymbol{y}\\ \boldsymbol{p},\boldsymbol{k}}} \tilde{S}(p)\tilde{S}(k)\mathrm{e}^{-\mathrm{i}(\boldsymbol{p}\cdot\boldsymbol{x}+\boldsymbol{k}\cdot\boldsymbol{y})} = \tilde{S}(E,\vec{0})\tilde{S}(E,\vec{0})$$

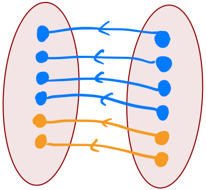

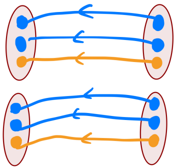

The Price

- Much more computationally demanding: $N_{SPSP} \sim (10 \text{ to } 100) N_{PP}$.

Contraction Algorithms

For Two Point Correlators

- Based on the unified contraction algorithm (Doi and Endres 2013) and the quark-level interpolating fields (Detmold and Orginos 2013).
- Employed the random field selection method (Li et al. 2021) to reduce spatial summation.[1]
- Further optimized for SPSP correlators. (Still in progress.)

[1] Implemented by Luchang Jin in the Qlattice library (`https://github.com/waterret/Qlattice`).

Contraction Algorithms

For Two Point Correlators

- Based on the unified contraction algorithm (Doi and Endres 2013) and the quark-level interpolating fields (Detmold and Orginos 2013).
- Employed the random field selection method (Li et al. 2021) to reduce spatial summation.[1]
- Further optimized for SPSP correlators. (Still in progress.)

For Three and Four Point Correlators

- Isospin rotation method & Sequential propagators
  $\Longrightarrow$ Two point correlation functions.

[1] Implemented by Luchang Jin in the Qlattice library (`https://github.com/waterret/Qlattice`).

Isospin Rotation Method

Basic Idea

- Strict SU(2) isospin symmetry in our lattice calculation.
- Wigner-Eckart theorem：

$$\begin{aligned} &\langle \alpha', j'm' | T_q^{(k)} | \alpha, jm \rangle \\ &= \langle jk; mq | jk; j'm' \rangle \frac{\langle \alpha', j' \| T^{(k)} \| \alpha, j \rangle}{\sqrt{2j+1}}, \end{aligned} \tag{1}$$

- Flavour-changing currents $\xrightarrow{\text{Isospin rotation}}$ Flavour-conserving currents
  $\Longrightarrow$ The same contraction structure as two point functions.

Isospin Rotation Method

Proton-Proton Fusion

- Initial state: $|I=1, I_3=1\rangle \equiv |1,1\rangle$, Final state: $|I=0, I_3=0\rangle \equiv |0,0\rangle$
- From W-E thm. & C-G coefficients:

$$\left\langle (d)^{I=0}_{I_3=0} \,\middle|\, \hat{O}^1_{-1} \,\middle|\, (pp)^{I=1}_{I_3=1} \right\rangle = -\left\langle (d)^{I=0}_{I_3=0} \,\middle|\, \hat{O}^1_0 \,\middle|\, (pn)^{I=1}_{I_3=0} \right\rangle . \tag{2}$$

Isospin Rotation Method

Proton-Proton Fusion

- Initial state: $|I = 1, I_3 = 1\rangle \equiv |1, 1\rangle$, Final state: $|I = 0, I_3 = 0\rangle \equiv |0, 0\rangle$
- From W-E thm. & C-G coefficients:

$$\left\langle (d)^{I=0}_{I_3=0} \middle| \hat{O}^1_{-1} \middle| (pp)^{I=1}_{I_3=1} \right\rangle = -\left\langle (d)^{I=0}_{I_3=0} \middle| \hat{O}^1_0 \middle| (pn)^{I=1}_{I_3=0} \right\rangle . \tag{2}$$

Double Beta Decay

- Initial state: $|I = 1, I_3 = -1\rangle \equiv |1, -1\rangle$, Final state: $|I = 1, I_3 = 1\rangle \equiv |1, 1\rangle$. Operator: $\hat{O}^2_2$, while $\hat{O}_0 = \hat{O}^2_0 + \hat{O}^0_0$
- Eliminating $\hat{O}^0_0$ by using $\left\langle pp \middle| \hat{O}_0 \middle| pp \right\rangle$ and $\left\langle pn(^1\mathrm{S}_0) \middle| \hat{O}_0 \middle| pn(^1\mathrm{S}_0) \right\rangle$.

$$\left\langle pp \middle| \hat{O}^2_2 \middle| nn \right\rangle = \frac{\sqrt{6}}{3} \left(\left\langle pp \middle| \hat{O}_0 \middle| pp \right\rangle - \left\langle pn(^1\mathrm{S}_0) \middle| \hat{O}_0 \middle| pn(^1\mathrm{S}_0) \right\rangle \right) . \tag{3}$$

Sequential Propagators

- Introducing sequential propagators.
  (For $(\overline{u}u - \overline{d}d)$ currents):

$$S'_u(x,y) = S(x,y) + \frac{\lambda}{\sqrt{2}} \int \mathrm{d}z S(x,z)\Gamma S(z,y),$$

$$S'_d(x,y) = S(x,y) - \frac{\lambda}{\sqrt{2}} \int \mathrm{d}z S(x,z)\Gamma S(z,y).$$

- λ terms $\rightarrow$ Three point correlators.
- λ^2 terms $\rightarrow$ Four point correlators.

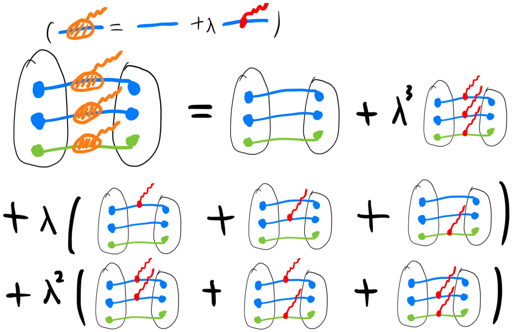

Extracting Matrix Elements

$$C_2(t) = \left\langle 0 \left| T\left\{ \mathcal{O}(t)\,(t')\,\mathcal{O}^\dagger(0) \right\} \right| 0 \right\rangle , \tag{4}$$

$$C_3(t) = \sum_{t'=0}^{T-1} \left\langle 0 \left| T\left\{ \mathcal{O}(t)\mathcal{J}\,(t')\,\mathcal{O}^\dagger(0) \right\} \right| 0 \right\rangle , \tag{5}$$

$$C_4(t) = \sum_{t'=0}^{T-1} \sum_{t''=0}^{T-1} \left\langle 0 \left| T\left\{ \mathcal{O}(t)\mathcal{J}\,(t')\,\mathcal{J}\,(t'')\,\mathcal{O}^\dagger(0) \right\} \right| 0 \right\rangle . \tag{6}$$

Extracting Matrix Elements

$$C_2(t) = \left\langle 0 \left| T \left\{ \mathcal{O}(t)\, (t')\, \mathcal{O}^\dagger(0) \right\} \right| 0 \right\rangle , \tag{4}$$

$$C_3(t) = \sum_{t'=0}^{T-1} \left\langle 0 \left| T \left\{ \mathcal{O}(t) \mathcal{J}\, (t')\, \mathcal{O}^\dagger(0) \right\} \right| 0 \right\rangle , \tag{5}$$

$$C_4(t) = \sum_{t'=0}^{T-1} \sum_{t''=0}^{T-1} \left\langle 0 \left| T \left\{ \mathcal{O}(t) \mathcal{J}\, (t')\, \mathcal{J}\, (t'')\, \mathcal{O}^\dagger(0) \right\} \right| 0 \right\rangle . \tag{6}$$

- The first order matrix elements can be extracted from the ratio $R_3(t)$:

$$R_3(t) = \frac{C_3(t)}{C_2(t)} = \frac{1}{2E_0} \langle f \mid J \mid i \rangle\, t + (\text{time independent terms}). \tag{7}$$

Extracting Matrix Elements

$$C_2(t) = \langle 0 \left| T \left\{ \mathcal{O}(t) \, (t') \, \mathcal{O}^\dagger(0) \right\} \right| 0 \rangle \, , \tag{4}$$

$$C_3(t) = \sum_{t'=0}^{T-1} \langle 0 \left| T \left\{ \mathcal{O}(t) \mathcal{J} \, (t') \, \mathcal{O}^\dagger(0) \right\} \right| 0 \rangle \, , \tag{5}$$

$$C_4(t) = \sum_{t'=0}^{T-1} \sum_{t''=0}^{T-1} \langle 0 \left| T \left\{ \mathcal{O}(t) \mathcal{J} \, (t') \, \mathcal{J} \, (t'') \, \mathcal{O}^\dagger(0) \right\} \right| 0 \rangle \, . \tag{6}$$

- The first order matrix elements can be extracted from the ratio $R_3(t)$:

$$R_3(t) = \frac{C_3(t)}{C_2(t)} = \frac{1}{2E_0} \langle f \,|\, J \,|\, i \rangle \, t + (\text{time independent terms}). \tag{7}$$

- Similarly, for the second order matrix elements:

$$R_4(t)\big|_{\text{t dep.}} = \frac{C_4(t)}{C_2(t)}\Big|_{\text{t dep.}} = \underbrace{\frac{\langle f \,|\, J \,|\, \alpha \rangle \langle \alpha \,|\, J \,|\, i \rangle}{8E_0 E_\alpha} t^2 \Big|_{E_\alpha \approx E_0}}_{\text{long-distance term}} + \underbrace{\sum_{E_\alpha \neq E_0} \frac{\langle f \,|\, J \,|\, \alpha \rangle \langle \alpha \,|\, J \,|\, i \rangle}{4E_0 E_\alpha (E_\alpha - E_0)} t}_{\text{short-distance term}} \tag{8}$$

Analysis of Lattice Calculations

Basic Information

Lattice Setup

- Action: Domain wall fermions + Iwasaki gauge action.
- 42 configurations for 24I & 235 configurations for 16I.
- Lattice information (From RBC/UKQCD) (Aoki et al. 2011; Boyle et al. 2016):

	β	$L^3 \times T$	am_l	$L(\text{fm})$	$a^{-1}(\text{GeV})$	$m_\pi(\text{MeV})$	Z_A
24I	2.13	$24^3 \times 64$	0.01	2.6496(73)	1.7844(49)	432.2(1.4)	0.71759(56)
16I	2.13	$16^3 \times 32$	0.01	/	/	/	/

Propagators

- 8 source locations for each even time slices (4 for sequential propagators).
- Applied the random field selection method after smearing. (Li et al. 2021)
  (For saving disk and the cost of spatial summation.)

Proton & Diproton Effective Mass (Preliminary)

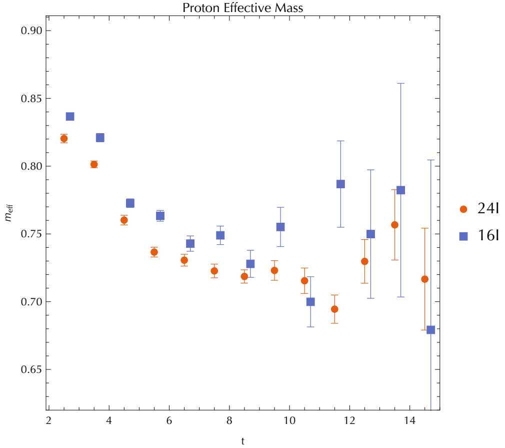

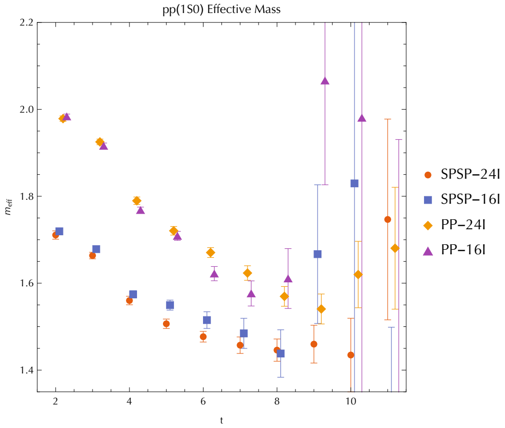

- Data from 24I with only 42 cfgs is even better than 16I with 235 cfgs.
- Excited states contamination has been significantly reduced in SPSP correlators.

Isotriplet & Isosinglet Mass Difference (Preliminary)

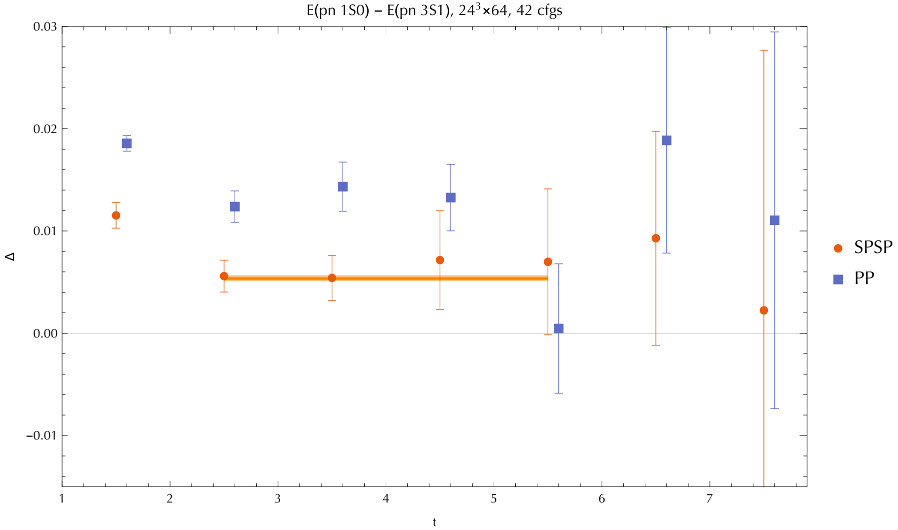

$$\Delta \equiv E_{\mathrm{pn(1S0)}} - E_{\mathrm{pn(3S1)}} = 0.0054(1). \tag{9}$$

g_A (Preliminary)

- Fitting result:

$$g_A = 1.198(26)$$

(at $m_\pi = 432.2(1.4)\mathrm{MeV}$)

- Consistent with RBC/UKQCD:

$$g_A = 1.186(36)$$

(With the same lattice setup)
(Yamazaki et al. 2008)

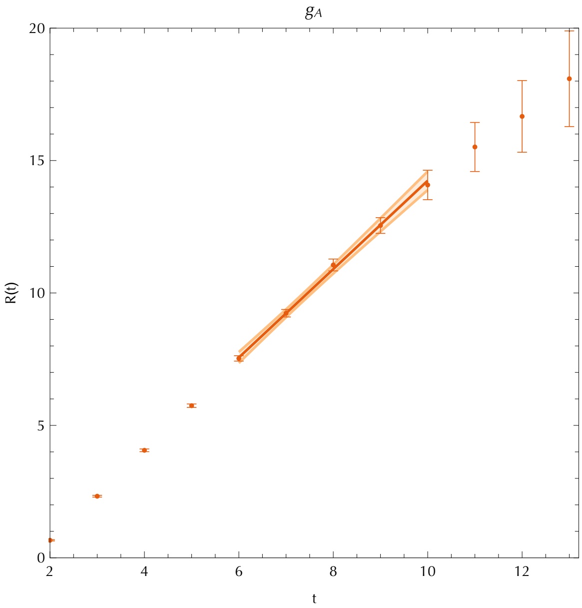

$pp \to d$ (Preliminary)

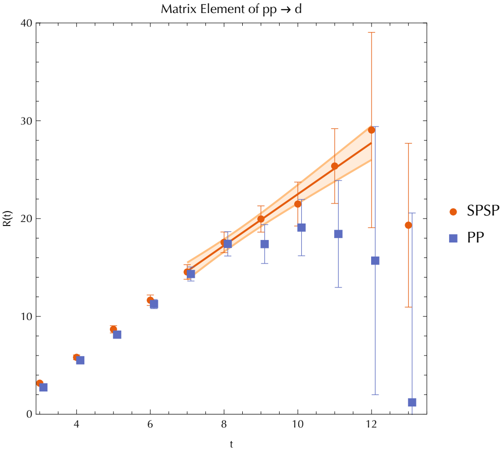

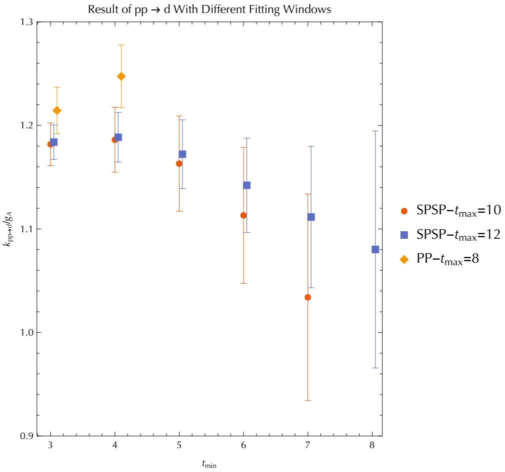

- Fitting by: $R(t) = \langle pp \,|\, \tilde{J}_3 \,|\, d \rangle \, t + b$
- Result: $\dfrac{\langle pp \,|\, \tilde{J}_3 \,|\, d \rangle}{g_A} = 1.11(7)$.
- Severe excited states contamination. $\to$ Multi-states fit (In progress)

$2\nu2\beta$ (Preliminary)

- Fitting by:
  $R(t) = (\text{long dist.})\frac{t^2}{2} + (\text{short dist.})t + C$
- Long-distance contribution:

$$\frac{\Delta}{g_A^2}\frac{\langle pp\,|\,\mathcal{J}\,|\,d\rangle\,\langle d\,|\,\mathcal{J}\,|\,nn\rangle}{\Delta} = 1.02(6).$$

- Short-distance contribution:

$$\frac{\Delta}{g_A^2}\sum_{l\neq d}\frac{\langle pp\,|\,\mathcal{J}\,|\,l\rangle\,\langle l\,|\,\mathcal{J}\,|\,nn\rangle}{\delta_l} = -0.065(5).$$

- Results by NPLQCD (Tiburzi et al. 2017) ($m_\pi \sim 806\,\mathrm{MeV}$):

$$(\text{long dist.}) = 1.00(3)(1),$$
$$(\text{short dist.}) = -0.04(4)(2).$$

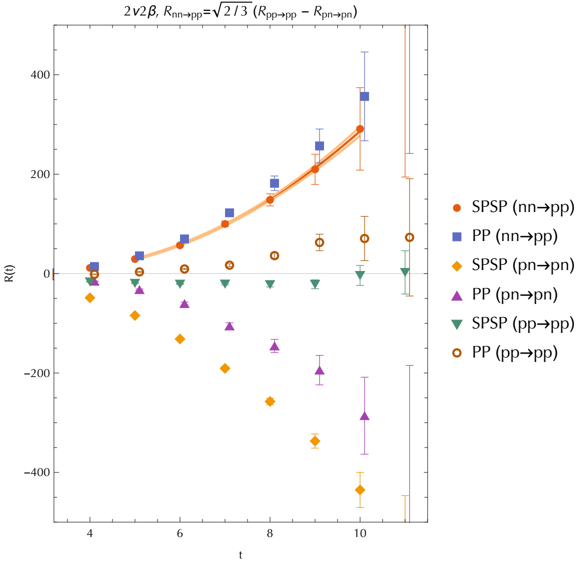

Ftting Window Comparison (Preliminary)

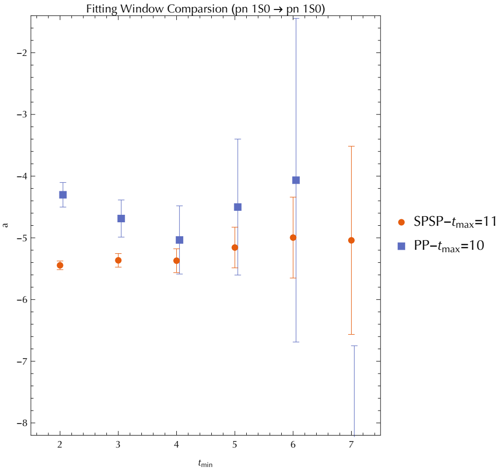

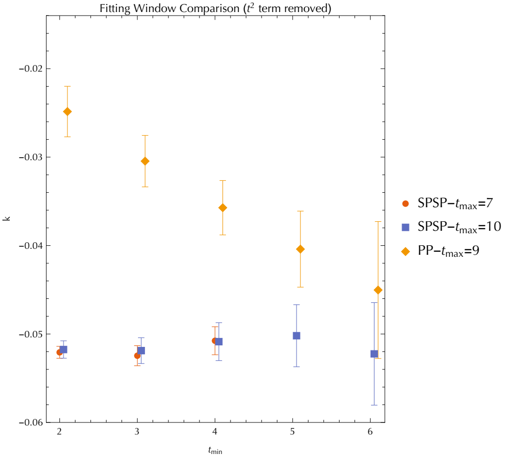

Summary & Prospectives

We presented

- Our method of calculating dibaryon weak transition matrix elements.
- Comparison of PP and SPSP correlation functions.
- Preliminary results of $pp \to d$ and $2\nu 2\beta$ matrix elements.

Summary & Prospectives

We presented

- Our method of calculating dibaryon weak transition matrix elements.
- Comparison of PP and SPSP correlation functions.
- Preliminary results of $pp \to d$ and $2\nu 2\beta$ matrix elements.

Prospectives

- Checking our results and performing a more complete error analysis.
- Including more configurations to reduce statistical uncertainties.
- Performing calculation on ensembles with larger lattice volume.
- Working for $0\nu 2\beta$ matrix elements.

Thanks For Your Attention.